

## 5-(1*H*-Benzimidazol-1-yl)-3-alkoxy-2-thiophenecarbonitriles as potent, selective, inhibitors of IKK- $\epsilon$ kinase

Paul Bamborough,<sup>a</sup> John A. Christopher,<sup>a,\*</sup> Geoffrey J. Cutler,<sup>b</sup> Marion C. Dickson,<sup>a</sup> Geoffrey W. Mellor,<sup>b</sup> James V. Morey,<sup>a,†</sup> Champa B. Patel<sup>b</sup> and Lisa M. Shewchuk<sup>c</sup>

<sup>a</sup>GlaxoSmithKline R&D, Medicines Research Centre, Gunnels Wood Road, Stevenage, Hertfordshire SG1 2NY, UK

<sup>b</sup>GlaxoSmithKline R&D, New Frontiers Science Park, Third Avenue, Harlow, Essex CM19 5AW, UK

<sup>c</sup>GlaxoSmithKline Inc., 5 Moore Drive, Research Triangle Park, NC 27709, USA

Received 21 August 2006; revised 4 September 2006; accepted 7 September 2006

Available online 25 September 2006

**Abstract**—The identification and hit-to-lead exploration of a novel, potent and selective series of substituted benzimidazole–thiophene carbonitrile inhibitors of IKK- $\epsilon$  kinase is described. Compound **12e** was identified with an IKK- $\epsilon$  enzyme potency of  $\text{pIC}_{50}$  7.4, and has a highly encouraging wider selectivity profile, including selectivity within the IKK kinase family.  
© 2006 Elsevier Ltd. All rights reserved.

Protein kinases catalyse the transfer of the  $\gamma$ -phosphate from ATP to the side-chain hydroxyl group of tyrosine, serine or threonine residues of proteins involved in the regulation of diverse cellular functions. Aberrant kinase activity is implicated in many diseases and makes this target class attractive for the pharmaceutical industry.<sup>1</sup>

The I $\kappa$ B (IKK) family of kinases represents an area of intense research, most of which has centred on inhibition of IKK- $\beta$  or the complex formed between the kinases IKK- $\alpha$  and IKK- $\beta$  and the regulatory sub-unit NEMO (also known as IKK-1, IKK-2 and IKK- $\gamma$ , respectively).<sup>2</sup> IKK- $\epsilon$  (also known as IKK-3, inducible IKK or IKK-i) was initially identified as an LPS-induced transcript from a macrophage cell-clone and later as part of a PMA-inducible I $\kappa$ B kinase complex, different from the classical IKK- $\alpha$ / $\beta$ /NEMO complex.<sup>3,4</sup> It was shown to be predominantly expressed in cells and tissues of the immune system (peripheral blood leukocytes, thymus and spleen) and constitutively expressed in human rheumatoid arthritis, osteoarthritis and normal synovium.<sup>5</sup> Several observations suggest that IKK- $\epsilon$  might be involved in the regulation of transcription factors, such as NF- $\kappa$ B, IRF3 and C/EBP, all of

which are known to be involved in the regulation of pro-inflammatory cytokines.<sup>3,6–11</sup> Inhibition of IKK- $\epsilon$  has been less widely explored than inhibition of IKK- $\beta$  or the classical IKK- $\alpha$ / $\beta$ /NEMO complex. Potent inhibitors of IKK- $\epsilon$  with selectivity within the IKK family will therefore be valuable in further clarifying the roles, and defining the therapeutic value, of this kinase target.

As part of a hit identification exercise, benzimidazole **1** was identified as a moderately potent inhibitor of IKK- $\epsilon$ ,  $\text{pIC}_{50}$  5.4 (Fig. 1).<sup>12</sup> Extensive in-house kinase cross-screening is routine within GSK, and substantial selectivity data were readily available for **1**. Analysis of these data revealed a moderate selectivity profile, with inhibition of Polo-like kinase 1 (PLK1,  $\text{pIC}_{50}$  6.9) being one of the most significant off-target activities. The PLK1 activity was not surprising, as **1** and analogues originated from in-house medicinal chemistry efforts targeted at this kinase. PLK1 has the potential to interfere with several stages of mitosis and therefore presents an intervention opportunity in the oncology arena.<sup>13</sup>

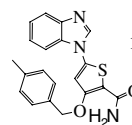


**Figure 1.** Initial hit compound **1**.

**Keywords:** IKK- $\epsilon$  kinase inhibitors; IKK.

\* Corresponding author. Tel.: +44 0 1438 763578; e-mail: [John.A.Christopher@gsk.com](mailto:John.A.Christopher@gsk.com)

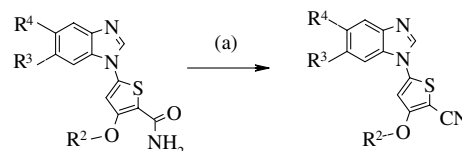
† Present address: University Chemical Laboratory, Lensfield Road, Cambridge CB2 1EW, UK.

**Table 1.** IKK- $\varepsilon$  and PLK1 inhibition of compounds **2–5**

Compound	R <sup>1</sup>	IKK-β pIC <sub>50</sub>	IKK-ε pIC <sub>50</sub>	PLK1 pIC <sub>50</sub>
<b>2</b>	CONH <sub>2</sub>	<4.8	<4.8	6.9
<b>3</b>	CN	<4.8	5.3	6.2
<b>4</b>	CONH <sub>2</sub>	<4.8	<4.8	6.6
<b>5</b>	CN	<4.8	6.1	<5.0

Identification of **1** and the availability of analogues from the PLK1 drug development effort prompted further screening of members of the series to gain a clearer picture of the IKK- $\epsilon$  structure–activity relationships and the wider kinase selectivity profile. From this exercise it became apparent, as illustrated by the two pairs of molecules in Table 1, Compounds **2–5**, that replacement of the amide moiety by a nitrile group was detrimental to the PLK1 activity, but beneficial to the inhibitory effect upon IKK- $\epsilon$ .<sup>14</sup> Furthermore, compounds **2–5** were observed to be inactive against IKK- $\beta$ .<sup>15</sup>

Encouraged by these early indications of selectivity, especially in the case of **5**, we sought to obtain a ligand-bound crystal structure to clarify the binding mode and aid our understanding of the origins of the selectivity. Although IKK- $\epsilon$  crystallography was not available, amide **6** showed modest CDK-2 inhibitory potency (pIC<sub>50</sub> 5.8). It was possible to soak this compound into crystals of CDK-2/cyclin A to obtain a structure of the complex.<sup>16</sup> The CDK-2 structure acted as a surrogate for IKK- $\epsilon$  and provided valuable information which could be translated, with knowledge of the amino acid differences in the ATP-binding sites, to aid our understanding of the binding mode in the target kinase. As illustrated in Figure 2, the structure shows that the characteristic hydrogen-bond from the Leu83 residue in the hinge region of the CDK-2 ATP-binding site is



**Scheme 1.** Reagents and condition: (a)  $(\text{F}_3\text{CCO})_2\text{O}$ , pyridine,  $\text{CH}_2\text{Cl}_2$ ,  $-10\text{ }^\circ\text{C}$ .

accepted by N3 of the benzimidazole ring. The dimethoxy substituents at the 5 and 6 positions of the benzimidazole ring point towards solvent at the edge of the ATP site. The benzimidazole also makes hydrophobic contacts with Ala31 and Leu134. The thiophene ring lies alongside the gatekeeper Phe80. An internal hydrogen-bond between the carboxamide NH<sub>2</sub> and the ether oxygen orientates the ether-linked R2 benzyl group (see [Scheme 1](#)) so that its plane lies perpendicular to the plane of the benzimidazole ring. The *ortho*-Cl atom makes hydrophobic contacts with Val18 and Gly11 on the N-terminal lobe. The opposite edge of the phenyl ring is in the region of the backbone carbonyl of Gln131 in the C-terminal lobe, although it makes no specific interactions. The primary carboxamide substituent on the thiophene ring points towards the back pocket of the active site, where it makes a direct hydrogen-bond with Glu51 via the NH<sub>2</sub>. However, the carbonyl of the carboxamide lacks any hydrogen-bonding partner protein atom or visible water.

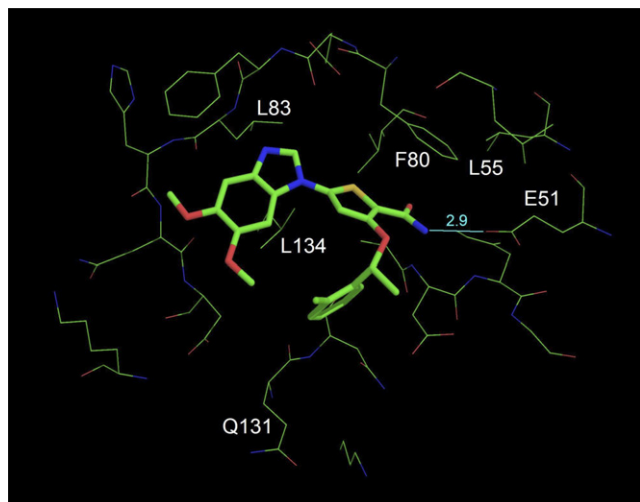
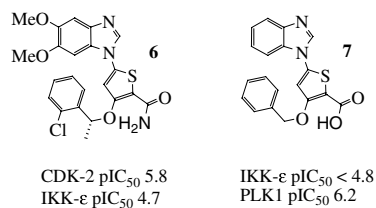


**Figure 2.** X-ray structure of compound **6** complexed with CDK-2/cyclin A.

It is believed that the binding mode of this series in IKK- $\epsilon$  is similar to that seen in CDK-2, and that N3 of the benzimidazole also forms a hydrogen-bond to the hinge region (Cys89 in IKK- $\epsilon$ ). Comparison of the sequences of IKK- $\epsilon$  and PLK1 in the context of the CDK-2 structure provides an explanation for the selectivity differences between amide and nitrile analogues in these kinases. A model of compound **12a** docked into a homology model of IKK- $\epsilon$  is illustrated in [Figure 3](#).<sup>17</sup>

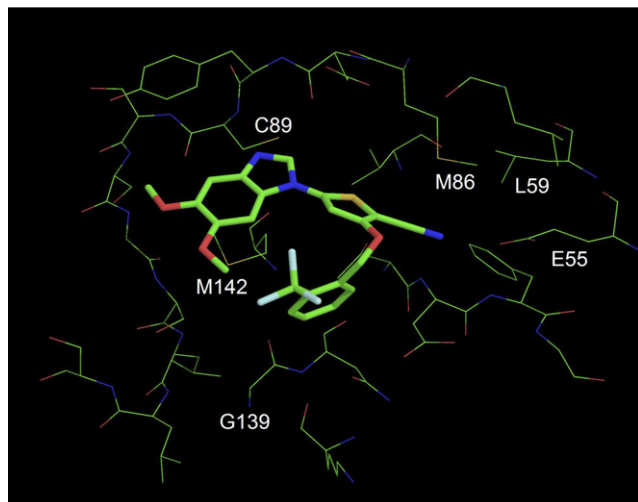


Figure 3. Compound **12a** docked into the homology model of IKK-ε.

Table 2 shows some of the aligned residues in the ATP-binding sites of CDK-2, IKK-ε, PLK1 and MK2. Especially relevant is the unusual histidine (His105) buried deep in the back of the ATP site of PLK1. It is much more common in protein kinases to find aliphatic residues at the equivalent position, for example Leu55 in CDK2 and Leu59 in IKK-ε. MK2, whose X-ray structure has been solved, has an analogous histidine (His108) at the same position as His105 in PLK1. The crystal structure of staurosporine bound to MK2 shows a water molecule buried at the back of the ATP site that appears to be hydrogen-bonded to both His108 and Glu104.<sup>18</sup> Since both residues are conserved in PLK1, we believe that a similar situation exists, and that in certain ligand-bound situations a water molecule can bridge between His105 and Glu101 at the back of the ATP site. It is striking that even carboxylic acids can be tolerated in the position of the amide in PLK1 (e.g., compound **7**), presumably because the ionisable histidine provides a counter to the charge.

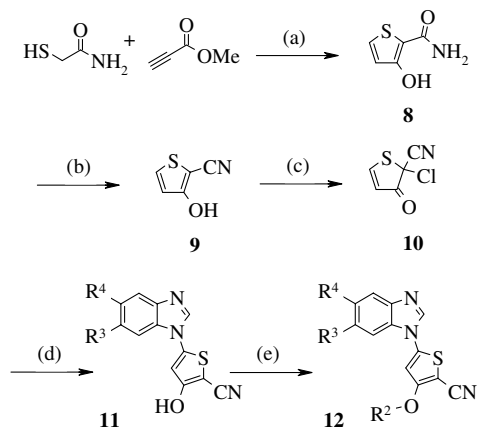
Replacement of the PLK1 His105 with leucine in both CDK-2 and IKK-ε means that the hydrogen-bonding potential of a water at the same position cannot be satisfied. Burial of water in this location in IKK-ε would therefore be expected to be less favourable than in PLK1, and so compounds that bind with a hydrogen-bond to this water are less potent. In contrast, com-

pounds such as **5**, where the amide is replaced by nitrile, lose much of their potential to hydrogen-bond to any buried water, and so are less potent against PLK1. It is believed that in the ATP-binding site of IKK-ε they displace any buried water and the cyano group fills the lipophilic cavity left behind.

A chemistry effort was initiated, with the aim of expanding the SAR, enhancing the IKK-ε potency and improving the selectivity profile. Two approaches were pursued in parallel; first, selections of available molecules with amide substitution on the thiophene were dehydrated to the corresponding nitrile, using trifluoroacetic anhydride in dichloromethane (Scheme 1). The precursor amides were prepared by routes previously reported.<sup>19</sup>

Alternatively, the nitrile moiety was installed at an early stage in the synthesis via the dehydration of 3-hydroxy-2-thiophenecarboxamide **8**, itself formed by the conjugate addition/cyclisation of 2-mercaptoacetamide onto methyl 2-propiolate (Scheme 2). With nitrile **9** in hand, installation of the benzimidazole portion was achieved via reaction with sulfonyl chloride and displacement of the intermediate chloride under conditions reported by Corral.<sup>20</sup> O-Alkylation under standard conditions then furnished target compounds **12**.

Key data are summarized below in Table 3. In most cases, R2 O-substitution was found to be beneficial to the IKK-ε activity, when compared to the unsubstituted hydroxy compound **12g**. O-Benzyl substitution appears to be generally more favourable than O-alkyl (compare **12a** to **5**, **12f**, **12h** and **12j**). Within the benzyl series, a significant preference for *ortho*-substitution on the phenyl ring is apparent, as illustrated by comparison of sulfones **12e** and **3**.  $\alpha$ -Branching of the benzyl chain in **12d** and **12l** is observed to be unfavourable (the (*S*)-enantiomers of **12d** and **12l** were not prepared), with a 10-fold drop in potency observed between **12a** and **12d**. This is interpreted to mean that there is a precise steric requirement which requires both *ortho* substitution on the ring and the absence of an  $\alpha$ -branch to position the benzylic phenyl ring in a suitable position.



Scheme 2. Reagents and conditions: (a) NaOMe, MeOH, 0 °C; (b) (F<sub>3</sub>CCO)<sub>2</sub>O, pyridine, CH<sub>2</sub>Cl<sub>2</sub>, rt; (c) Cl<sub>2</sub>SO<sub>2</sub>, CHCl<sub>3</sub>, rt; (d) substituted benzimidazole, triethylamine, CHCl<sub>3</sub>, rt; (e) alkyl bromide, K<sub>2</sub>CO<sub>3</sub>, DMF, 100 °C, microwave heating.

Table 2. ATP site comparison between human CDK-2, IKK-ε, PLK1 and MK2

CDK-2	IKK-ε	PLK1	MK2
ILE10	LEU15	LEU59	LEU70
VAL18	VAL23	CYS67	VAL78
ALA31	ALA36	ALA80	ALA91
LEU55	LEU59	HIS105	HIS108
VAL64	VAL68	VAL114	VAL118
PHE80	MET86	LEU130	MET138
LEU83	CYS89	CYS133	LEU141
GLN131	GLY139	GLY180	GLU190
LEU134	MET142	PHE183	LEU193
ALA144	THR156	GLY193	THR206

**Table 3.** IKK- $\epsilon$  inhibition values

Compound	R <sup>2</sup>	R <sup>3</sup>	R <sup>4</sup>	IKK- $\epsilon$ pIC <sub>50</sub>
<b>3</b>	–CH <sub>2</sub> (4-SO <sub>2</sub> MePh)	OMe	OMe	5.3
<b>5</b>	( $\pm$ )–CH <sub>2</sub> (2-Tetrahydrofuranyl)	H	H	6.1
<b>12a</b>	–CH <sub>2</sub> (2-CF <sub>3</sub> Ph)	OMe	OMe	6.6
<b>12b</b>	–CH <sub>2</sub> (2-CF <sub>3</sub> Ph)	OMe	O(CH <sub>2</sub> ) <sub>2</sub> -4-Morpholine	7.3
<b>12c</b>	–CH <sub>2</sub> (2-CF <sub>3</sub> Ph)	OMe	O(CH <sub>2</sub> ) <sub>3</sub> OH	7.6
<b>12d</b>	( <i>R</i> )-CHMe(2-CF <sub>3</sub> Ph)	OMe	OMe	5.4
<b>12e</b>	–CH <sub>2</sub> (2-SO <sub>2</sub> MePh)	OMe	OMe	7.4
<b>12f</b>	–(CH <sub>2</sub> ) <sub>2</sub> -4-Morpholine	OMe	OMe	5.8
<b>12g</b>	H	OMe	OMe	5.6
<b>12h</b>	–CH <sub>2</sub> -Cyclopropyl	OMe	OMe	5.5
<b>12i</b>	–CH <sub>2</sub> Ph	H	H	6.0
<b>12j</b>	–(CH <sub>2</sub> ) <sub>2</sub> -1-Piperidine	OMe	OMe	5.3
<b>12k</b>	–CH <sub>2</sub> (4-CONH <sub>2</sub> Ph)	OMe	OMe	4.9
<b>12l</b>	( <i>R</i> )-CHMe(2-ClPh)	OMe	OMe	5.8

**Table 4.** Kinase inhibitory potencies of **12e** (values in pIC<sub>50</sub>)

Alk-5	EGFR	ErbB2	GSK-3	IKK- $\alpha$	IKK- $\beta$	IKK- $\epsilon$	Jnk-3	p38 $\alpha$	p38 $\beta$	PLK1
<5.3	<5.0	<5.0	<4.8	<4.8	<4.8	7.4	<4.8	<4.8	<4.8	6.1

In most cases, the R<sup>3</sup> and R<sup>4</sup> substituents are identical in this initial exploration of the SAR. From the CDK-2 crystal structure, which shows R<sup>3</sup> and R<sup>4</sup> pointing towards solvent, it was anticipated that modifications incorporating solubilising groups to alter the physico-chemical properties of the series would be well tolerated in these positions. Comparison of **12b** and **12c** with **12a** shows that this is the case, and in fact longer chains give an increase in IKK- $\epsilon$  activity, perhaps because of lipophilic interactions with Leu15 and other residues around the edge of the ATP site.

In addition to the highly encouraging IKK- $\epsilon$  inhibitory characteristics of the compounds, in-house cross-screening indicated that an excellent overall kinase selectivity profile was maintained, a key finding being that all compounds in Table 3 were essentially inactive (pIC<sub>50</sub> < 4.8) at IKK- $\alpha$  and IKK- $\beta$ . Kinase data are summarized above in Table 4 for **12e**, which also has encouraging developability characteristics; specifically good aqueous solubility (60  $\mu$ M) and inactivity (pIC<sub>50</sub> < 4.3) against the cytochrome P450 isozymes 1A2, 2D6, 2C9 and 3A4.

In summary, the 5-(1*H*-Benzimidazol-1-yl)-3-alkoxy-2-thiophenecarbonitrile series represents a novel, potent and selective class of IKK- $\epsilon$  inhibitors. The most potent compounds obtained are **12b**, **12c** and **12e**, with enzyme inhibitory potencies of pIC<sub>50</sub> 7.3, 7.6 and 7.4, respectively. The series has excellent selectivity against IKK- $\alpha$  and IKK- $\beta$ , and provides an opportunity to examine the therapeutic role of IKK- $\epsilon$  and further aid the understanding of the IKK family of kinases.

### Acknowledgments

The GSK Screening and Compound Profiling and Computational, Analytical and Structural Sciences groups are thanked for the generation of kinase inhibition data, and for solubility and P450 data for **12e**. The authors

also thank Karen E. Lackey and David D. Miller for their guidance and support, and synthetic contributions from James A. Linn, Kristen E. Nailor, Kevin W. Kuntz and James M. Salovich are gratefully acknowledged. Duncan B. Judd and Bethany Brown are thanked for their assistance in the large-scale synthesis of **9**.

### References and notes

- Parang, K.; Sun, G. *Curr. Opin. Drug Disc. Dev.* **2004**, *7*, 617.
- Coish, P. D. G.; Wickens, P. L.; Lowinger, T. B. *Expert Opin. Ther. Patents* **2006**, *16*, 1.
- Shimada, T.; Kawai, T.; Takeda, K.; Matsumoto, M.; Inoue, J.-i.; Tatsumi, Y.; Kanamaru, A.; Akira, S. *Int. Immunol.* **1999**, *11*, 1357.
- Peters, R. T.; Liao, S.-M.; Maniatis, T. *Mol. Cell* **2000**, *5*, 513.
- Aupperle, K. R.; Yamanishi, Y.; Bennett, B. L.; Mercurio, F.; Boyle, D. L.; Firestein, G. S. *Cell Immunol.* **2001**, *214*, 54.
- Nomura, F.; Kawai, T.; Nakanishi, K.; Akira, S. *Genes Cells* **2000**, *5*, 191.
- Sankar, S.; Chan, H.; Romanow, W. J.; Li, J.; Bates, R. J. *Cell. Signal.* **2006**, *18*, 982.
- Fitzgerald, K. A.; McWhirter, S. M.; Faia, K. L.; Rowe, D. C.; Latz, E.; Golenbock, D. T.; Coyle, A. J.; Liao, S.-M.; Maniatis, T. *Nat. Immunol.* **2003**, *4*, 491.
- Sharma, S.; tenOever, B. R.; Grandvaux, N.; Zhou, G.-P.; Lin, R.; Hiscott, J. *Science* **2003**, *300*, 1148.
- McWhirter, S. M.; Fitzgerald, K. A.; Rosains, J.; Rowe, D. C.; Golenbock, D. T.; Maniatis, T. *Proc. Natl. Acad. Sci. U.S.A.* **2004**, *101*, 233.
- Kravchenko, V. V.; Mathison, J. C.; Schwamborn, K.; Mercurio, F.; Ulevitch, R. J. *J. Biol. Chem.* **2003**, *278*, 26612.
- pIC<sub>50</sub> = –log<sub>10</sub> IC<sub>50</sub>; where the IC<sub>50</sub> is the concentration of compound required to inhibit the kinase activity by 50%. IKK- $\epsilon$  inhibition data were generated as follows: recombinant human IKK- $\epsilon$  was expressed in baculovirus as a FLAG-tagged fusion protein, and its activity assessed using a time-resolved fluorescence resonance energy transfer

(TR-FRET) assay. Briefly, IKK- $\epsilon$  (15 nM total protein) diluted in assay buffer (50 mM HEPES, 10 mM MgCl<sub>2</sub>, 1 mM Chaps, 1 DTT and 0.01% w/v BSA, pH7.4) was added to wells containing various concentrations of compound or DMSO vehicle (3% final). The reaction was initiated by the addition of 15  $\mu$ l of GST-I $\kappa$ B $\alpha$  substrate (25 nM)/ATP (2  $\mu$ M) in a total volume of 30  $\mu$ l. The reaction was incubated for 15 min at ambient temperature and then stopped by the addition of 15  $\mu$ l of 50 mM EDTA. Detection reagent (15  $\mu$ l) in buffer (100 mM Hepes, 150 mM NaCl, 0.1% w/v BSA, pH 7.4) containing antiphosphoserine-I $\kappa$ B $\alpha$ -32/36 monoclonal antibody, Clone 12C2 (Cell Signalling Technology, Beverly, Massachusetts, USA) labelled with W-1024 europium chelate (Perkin-Elmer, Turku, Finland) and an allophycocyanin labelled anti-GST antibody (Prozyme, San Leandro, California, USA) was added and the reaction further incubated for at least 45 min at ambient temperature. The degree of phosphorylation of GST-I $\kappa$ B $\alpha$  was measured using a Packard Discovery plate reader (Perkin-Elmer Life Sciences, Beaconsfield, UK) as a ratio of specific 665 nm energy transfer signal to reference europium 620 nm signal. The error of the assay is estimated as  $\pm 0.3$  log units, based on the standard deviation around the mean value of an inhibitor used as a standard compound in every assay.

13. Barr, F. A.; Silljé, H. H. W.; Nigg, E. A. *Nat. Rev. Mol. Cell Biol.* **2004**, *5*, 429.
14. PLK1 kinase activities were determined using methods described below.<sup>19a</sup>
15. IKK- $\beta$  kinase activities were determined using methods previously described; see: Baldwin, I. R.; Bamborough, P.; Christopher, J. A.; Kerns, J. K.; Longstaff, T.; Miller, D. D. Int. Patent Appl. WO 05/067923.
16. The PDB deposition code for this structure is 2I40. The expression, purification and crystallization of CDK-2/Cyclin A was carried out as previously described; see: Jeffrey, P. D.; Russo, A. A.; Polyak, K.; Gibbs, E.; Hurwitz, J.; Massagué, J.; Pavletich, N. P. *Nature* **1995**, *376*, 313. Crystals were soaked with 50  $\mu$ M compound for 2 days prior to data collections. The structure was refined to an Rfactor of 20% at 2.75 Å.
17. The sequence of IKK- $\epsilon$  was aligned to a large panel of protein kinase structures. CDK-2 was chosen as the template despite its relatively low sequence similarity (24% identity over the kinase domain) because of the availability of CDK-2 crystal structures complexed with molecules of interest. The kinase chain was extracted from a complex of CDK-2 with Cyclin A to give an active-like ATP site conformation. MODELLER (Sali, A.; Blundell, T. L. *J. Mol. Biol.* **1993**, *234*, 779) was used to generate IKK- $\epsilon$  coordinates. Limited refinement, in the presence of a manually bound ligand from a different chemical series to the one described here, was performed using Discover running through InsightII (Accelrys, [www.accelrys.com](http://www.accelrys.com)).
18. Underwood, K. W.; Parris, K. D.; Federico, E.; Mosyak, L.; Czerwinski, R. M.; Shane, T.; Taylor, M.; Svenson, K.; Liu, Y.; Hsiao, C.-L.; Wolfrom, S.; Maguire, M.; Malakian, K.; Telliez, J.-B.; Lin, L.-L.; Kriz, R. W.; Seehra, J.; Somers, W. S.; Stahl, M. L. *Structure* **2003**, *11*, 627.
19. (a) Andrews, C. W. III.; Cheung, M.; Davis-Ward, R. G.; Drewry, D. H.; Emmitte, K. A.; Hubbard, R. D.; Kuntz, K. Int. Patent Appl. WO 04/014899; (b) Cheung, M.; Emmitte, K. A. Int. Patent Appl. WO 05/037827.
20. Corral, C.; Lissavetzky, J. *Synthesis* **1984**, 847.